Anisotropic velocities and offset vector tile prestack-migration processing of the Durham Ranch 3D, Northwest Colorado

Scott Schapper, Robert Jefferson, and Alexander Calvert, Ion Geophysical
Marty Williams, East Resources

This article describes the anisotropic P-wave processing and resulting velocity attributes of the Durham Ranch 3D Firefly survey in the southern Sand Wash Basin of northwest Colorado (Figure 1). The goal of the seismic effort at Durham Ranch is to provide a clearer 3D image of the structures that may influence reservoir fracturing and capture anisotropy attributes that can be related to the local distribution of these fractures. With structural dip greater than 10° in portions of the reservoir, accurate imaging and properly positioned anisotropy information requires prestack migration. The high-density spatial coverage achieved in the Durham Ranch shoot afforded an opportunity to migrate in a domain that preserves a wide-azimuthal distribution of prestack data for anisotropy analysis. Improved imaging and positioning of the anisotropy attributes provides a clearer (perhaps causal) relationship between local deformation and fracturing, thus aiding in the selection of productive well locations and/or stimulation methods.

Geologic setting

The Sand Wash Basin is the southeastern-most sub-basin of the Greater Green River Basin complex—a prolific hydrocarbon province in the Rocky Mountains. The modern configuration of the Greater Green River Basin complex was established during the Late Cretaceous Laramide orogeny. This mountain-building event is characterized by basement-cored uplifts of the entire Lower Paleozoic through Upper Cretaceous sedimentary section that often form anticlinal closures which represented many early conventional exploration targets. Modern exploration activity in the basin complex has focused on hydraulic fracture stimulation of tight-gas sands and oil shales. Optimal drilling locations for these unconventional reservoirs are believed to be where fracture networks are naturally enhanced or readily augmented by hydraulic stimulation, so proximity to Laramide (or post-Laramide) deformation zones will increase the likelihood of encountering natural fracturing.

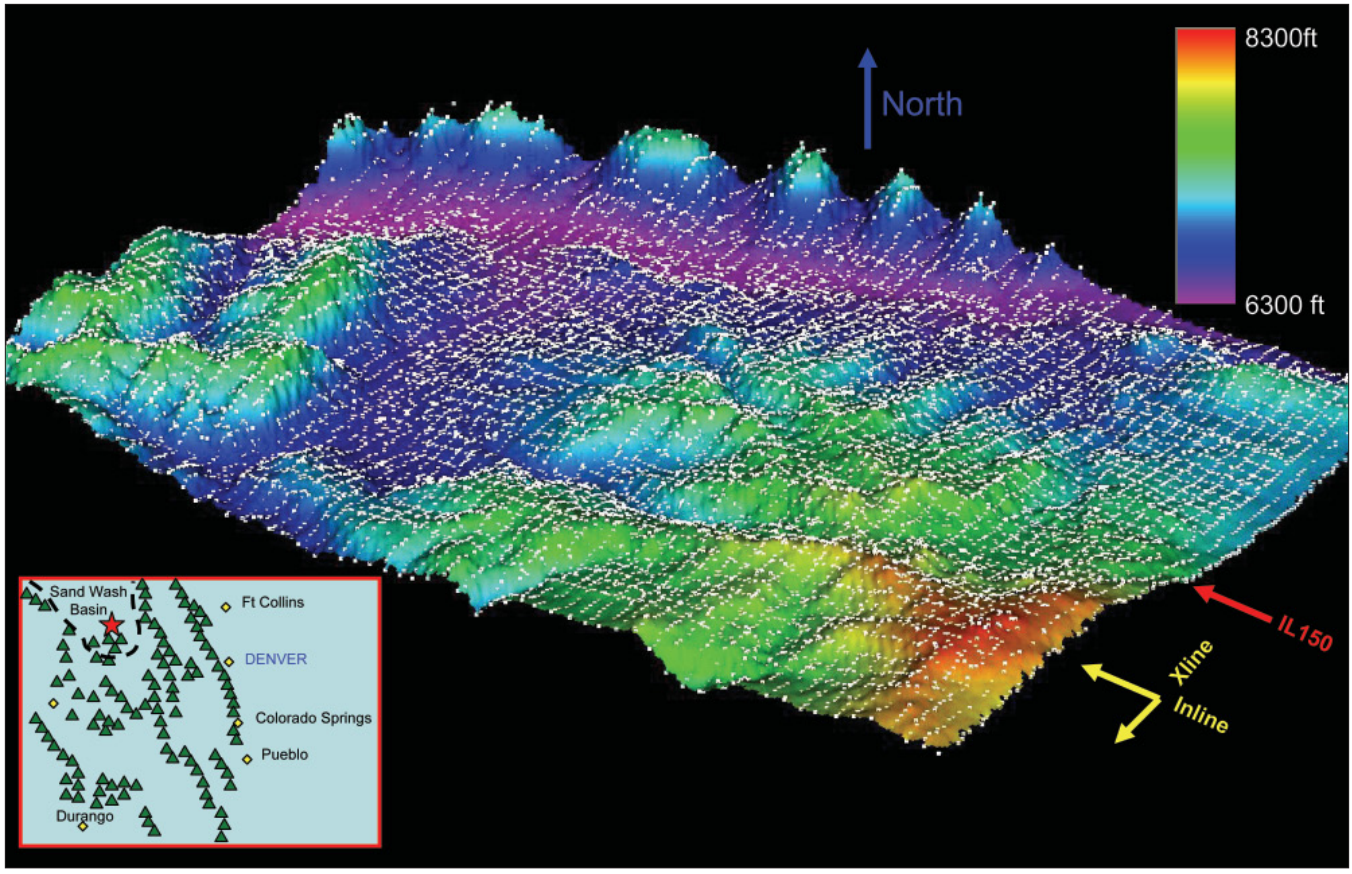

Figure 1. *Shot and receiver locations (white dots) of the Durham Ranch 3D survey overlain on topography. Continuous orthogonal coverage was attained at 165-ft source and receiver spacing in terrain with 2000 ft of topographic variation. Inset map of Colorado shows dashed outline of Sand Wash Basin and survey location (red star).*

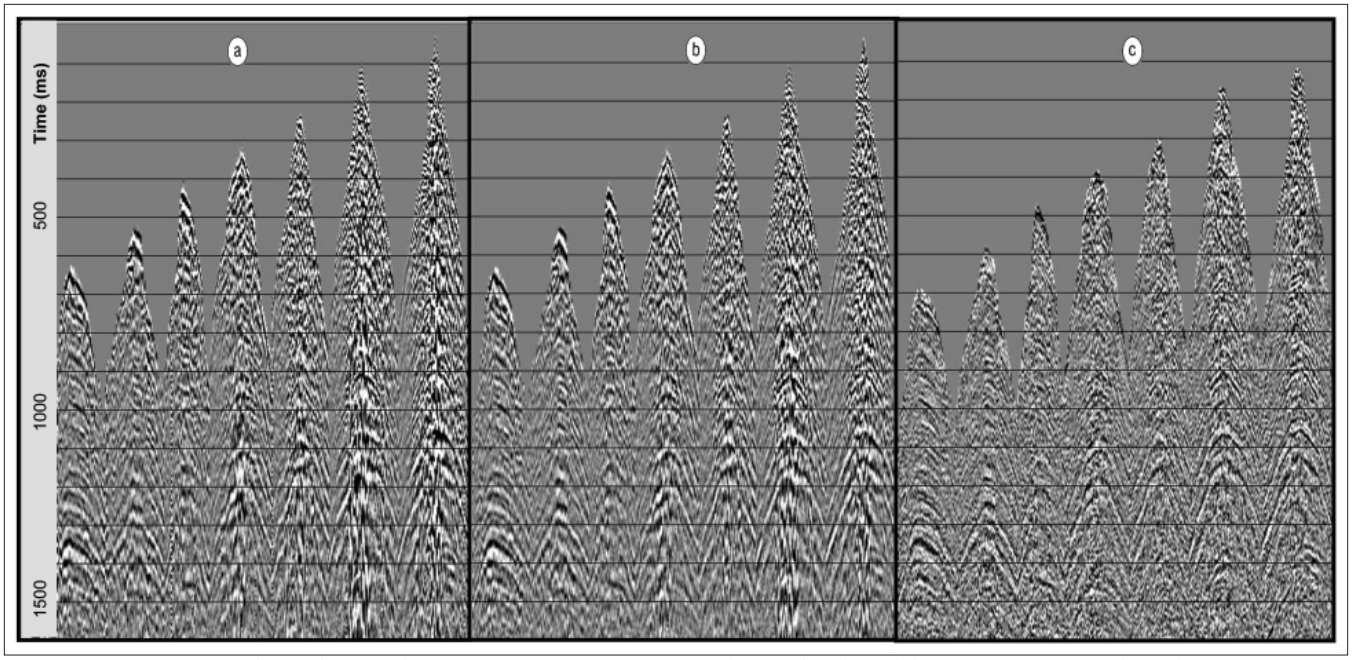

Figure 2. *Representative shot gather signal processing progression: (a) raw gathers with spherical divergence correction, (b) with noise attenuation, and (c) with deconvolution*

The Waddle Creek oil field in Moffat County, Colorado is atop a NW-SE striking Laramide anticline on the southern margin of the Sand Wash Basin. Analysis of borehole and existing 2D seismic data suggested that, in addition to Laramide compressional/transpressional deformation, the structure has also experienced more recent extensional stresses that are believed to be in response to Neogene relaxation of the Laramide event. Existing production at Waddle Creek Field has not yet taken advantage of predrill identification of natural fracturing with 3D attributes, thus providing an opportunity to significantly enhance production from the existing oil shale reservoir and potential prospects in deeper formations. The Waddle Creek area sedimentary section ranges from Paleozoic carbonates through Upper Cretaceous Niobrara shale; the post-Niobrara Cretaceous sediments have been eroded off the top of the anticline, resulting in a breached core of Niobrara shale exposed at the surface with the overlying Williams Fork sandstones of the Mesaverde Group forming cliffs on the north side of the anticline (Figure 1).

3D seismic design and acquisition

Detection of in-situ vertical fractures with seismic techniques relies on the measurement of seismic attributes that vary with azimuth (i.e., the rock properties that affect the transmission or reflection of seismic energy are directionally dependent). In order to measure such properties, a seismic survey should be designed to acquire data with as well sampled offsets and azimuths as is economically practical for prospective targets. In land acquisition, this often requires large channel counts in the field and adequate sampling can still be compromised by local access restrictions, topographic challenges, and environmental concerns.

The Durham Ranch 3D at Waddle Creek oil field manifested all of these challenges in abundance. To accurately measure azimuthal attributes for fractured reservoir targets ranging from 2000 to 7500 ft, the 30 square mile survey was designed as a dense, orthogonal grid of shot and receiver lines with a 3000-channel, wide-azimuth recording patch. The acquisition demands of such a high channel count were compounded by terrain exhibiting 2000 ft of vertical relief that ranged from irrigated farmland to exposed cliffs, cultural obstructions, and wildlife regulations. The terrain is so rough that approximately 70% of the survey area is only accessible by helicopter, which also dictated the use of explosive sources. These obstacles created operational complexity for tradition-

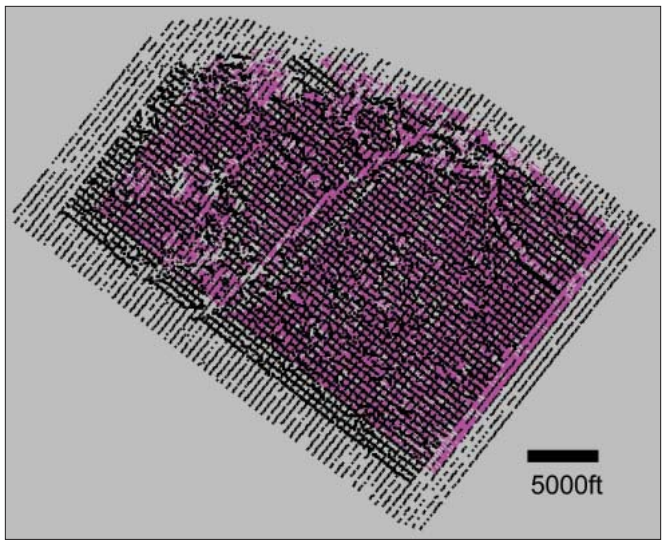

Figure 3. *Shot and receiver locations (black dots) overlain on vector-offset (OVT) cube fold (magenta = 1) for offset range 3000-4000 ft and azimuth of 82°. OVT cubes such as this are migrated separately in a manner analogous to common-offset cubes for traditional PSTM. Note that the gaps in OVT coverage are offset from the actual cultural obstructions.*

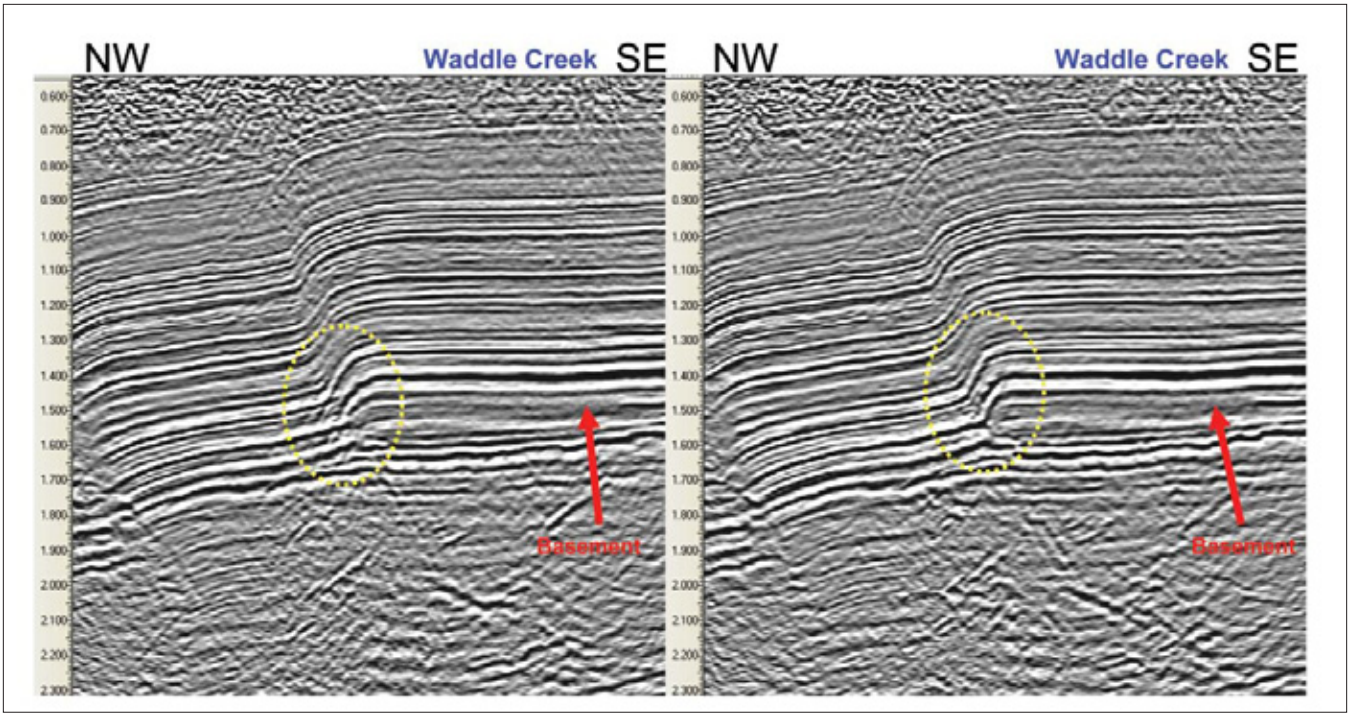

Figure 4. *OVT prestack time migrations of line 150. The isotropic migration on the left does not fully image the buried focus at 1.5 s. The layer anisotropic migration (η = 0.1) on the right properly images the buried focus, revealing what appears to be sediments folded atop faulted basement.*

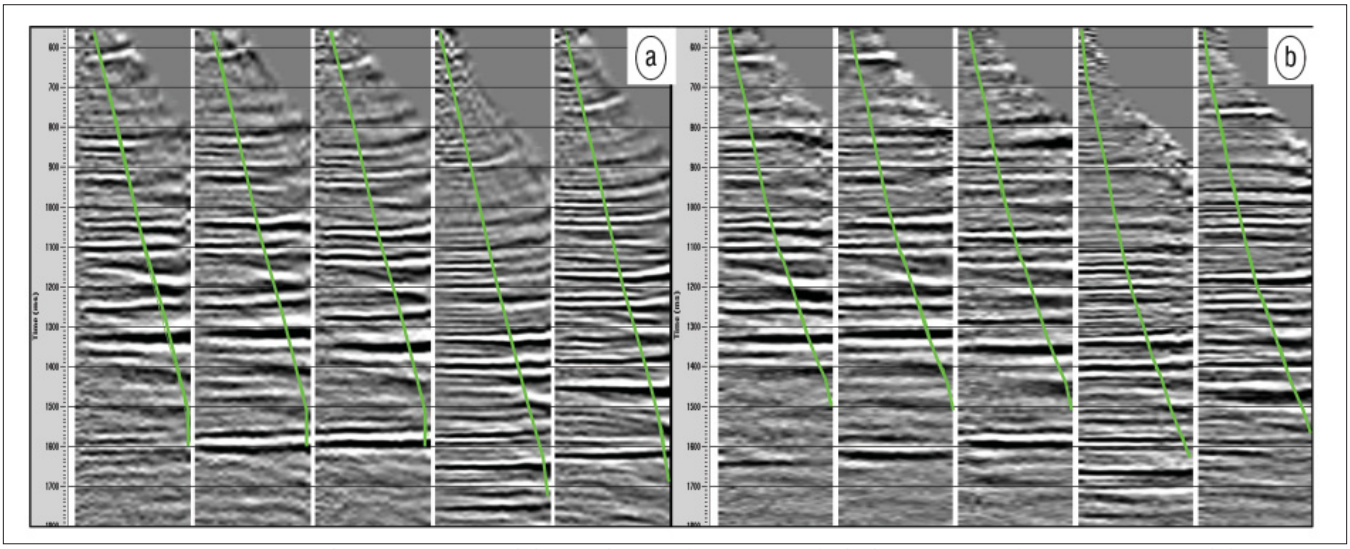

Figure 5. *Representative CDP gathers: (a) unmigrated data with normal moveout applied, (b) OVT prestack time migration with layer anisotropy term eta (η) = 0.1 properly flattens the higher-order moveout seen on the furthest offsets. The change in appearance of the deeper events shown is due to the positional changes in migration. For reference, the green curve represents an offset-to-depth ratio of 1.0.*

al cabled recording systems, but deployment of a cableless system allowed both the imaging objectives and acquisition challenges to be met. Chitwood et al. (2009) describe in more detail the imaging, logistical, and equipment demands that led to the selection of ION's Firefly cableless recording system for this survey.

The Durham Ranch 3D was acquired over 20 days in late 2008, yielding 9.2 million traces of high-quality seismic data from approximately 10,500 unique receiver points. Figure 1 illustrates the impressive coverage that was achieved under such difficult environmental circumstances.

Premigration processing

Data processing prior to prestack time migration employed well-established workflows that have proven effective for Greater Green River Basin 3D P-wave projects in terms of high-frequency content, effective long- and short-wavelength static solutions, high signal-to-noise ratio, and accurate velocities. This premigration processing flow employed labor-intensive attention to details while avoiding multichannel filtering techniques that might obscure traveltime or amplitude details in the signal. The general premigration processing steps included:

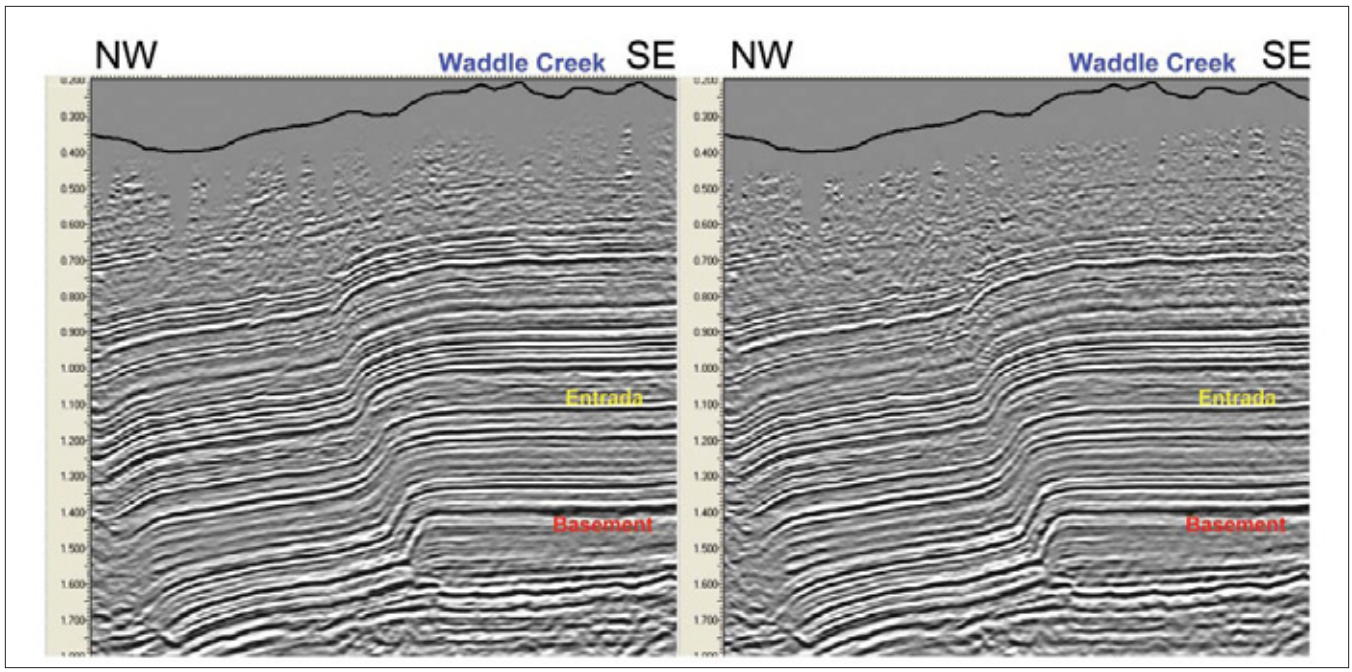

Figure 6. *Comparison of common-offset (left) and OVT (right) anisotropic prestack time migrations for line 150. Both migrations account for layer anisotropy with n = 0.1. The two images are comparable in the deep section, but the OVT image appears to suffer more from shallow sampling deficiencies.*

- refraction statics (single-layer delay time solution)
- first-pass hand-picked stacking velocities (1 × 1-mile grid)
- first-pass surface-consistent residual statics
- noise removal and time-variant spiking deconvolution
- second-pass hand-picked velocities (1/2 × 1/2-mile grid)
- second-pass surface-consistent residual statics

Removal of ground roll and other unwanted noise was accomplished via a combination of two processing techniques. The first technique analyzed the traces over time, space, and frequency windows. In this domain, signatures identified as anomalous relative to signal are attenuated within the frequency domain. This method removes anomalous spikes and noise bursts and attenuates some of the strongest portions of any ground roll present. The second technique attacks ground roll and air-blast noise more directly by employing an *f-x* domain filter targeted to attenuate linearly coherent energy at specific velocities and frequencies. The noise estimate provided by this filter is then subtracted from the input data to avoid the spatial smearing of amplitudes that would occur if the attenuation were to occur prior to an inverse transform.

Deconvolution of the noise-attenuated data was accomplished with a standard spiking operator designed over 1000-ms overlapping windows on an individual trace. In effect, this represents an aggressive signal whitening agent that attempts to account for time-variant Q. This time-variant spiking deconvolution has been found to provide a spatially consistent phase match to well data in the Greater Green River Basin. Due to the relatively uniform surface conditions provided by the Niobrara shale over most of the Durham Ranch 3D, ground-roll contamination was never a major processing obstacle. Figure 2 illustrates that the combination of noise removal and deconvolution effectively removed the bulk of the coherent noise while significantly improving the signal bandwidth.

Offset vector tile (OVT) processing

In the presence of significant geologic dip, premigration analysis of velocity anisotropy can be difficult as dip and azimuthal anisotropy have the same azimuthal NMO signature. Geologic dips of greater than 12–14° will impart azimuthal P-wave time shifts that exceed that of the typical 3% azimuthal anisotropy found in most continental basins containing well-consolidated sediments (Williams and Jenner, 2002). As one would prefer to remove any first-order dip effects prior to measuring/correcting the azimuthal time shifts, prestack migration is desired. Unfortunately, standard common-offset prestack migration techniques do not preserve azimuthal information, rendering any subsequent azimuthal analysis impossible. A common approach that attempts to address this problem is to perform individual prestack migrations on azimuth sectors of the data. However, this sectoring method can produce noisy prestack images owing to limited fold within the sectors and often requires large sectors leading to poor statistics for analysis of anisotropic properties (Lynn, 2007).

An alternative to sectoring is to migrate into vector-offset bins, as opposed to the scalar offset bins that are traditionally used for common-offset prestack migration (e.g., Calvert et al., 2008). Around 1999, this approach was independently proposed almost simultaneously by Peter Cary as the *common offset vector* (COV) and Gijs Vermeer under the more publicized name *offset vector tile* (OVT). If a survey is ac-

quired with sufficient spatial coverage of these vector-offset bins (henceforth referred to as OVT), a full volume containing data of approximately constant offset and azimuth can be built (Figure 3). Many of these vector-offset volumes can be individually migrated, thus creating migrated data that preserve offset and azimuth for azimuthal analysis (e.g., Calvert, et al., 2008). With tight line spacing, relatively coarse source and receiver spacing, and an orthogonal geometry, the Durham Ranch 3D was designed with OVT processing in mind. The spatial coverage of vector-offset bins in this survey is good for many offsets and azimuths. Recent OVT processing of other modern surveys that were not designed for OVT has shown that the method can accommodate less than optimal sampling in some cases.

Prestack time migration

An isotropic velocity field suitable for prestack time migration was created by prestack time migration (PSTM) of common-offset data with smoothed stacking velocities and outputting target locations on a 1/2 x 1/2 mile grid. Subsequent velocity analysis, interpolation, and smoothing yielded imaging velocities independent of dip effects.

The initial OVT PSTM with this isotropic velocity field (Figure 4a, line 150) resulted in a significant imaging improvement local to the fault zone in the middle of the survey when compared to earlier poststack time migrations. This zone represents a lateral ramp that splays off the main field-bounding fault to the southwest of the survey and is of particular interest as it may represent an area of enhanced fracturing within the existing Waddle Creek Field. Unfortunately, the PSTM image does not resolve the buried focus in the deeper portion of the ramp zone (1.5 s) as evidenced by the remnant "bow tie."

Examination of the velocity field and output gathers did not suggest that the isotropic velocity field was in error; therefore, anisotropic traveltime effects may need to be accounted for in migration to properly image the fault zone. It had been noted early in the processing that significant higher-order moveout was present at further offsets (Figure 5a) even when ray curvature effects are included in the migration. This higher-order moveout is usually a manifestation of layer anisotropy and can be adequately corrected by adding the higher-order eta (η) parameter to the normal moveout equation. Trial moveout and stack tests revealed that an eta value of 0.1 was effective in correcting the layer anisotropy traveltime effects for the entire sedimentary section at Durham Ranch.

A subsequent iteration of OVT PSTM with the inclusion of the layer anisotropy term (η = 0.1) yielded a much improved image of the buried focus in the fault zone (Figure 4b). Examination of the output gathers (Figure 5b) confirms that this migration properly flattened the events at the further offsets.

The significantly improved structural image of the fault zone in Figure 5b provides a clearer picture of the local sedimentary response to the uplifted basement. On this particular line, it remains unclear whether the faulting extends into sediments or the sediments are merely flexed in response to the basement uplift.

Another interesting geologic feature found on Figure 4b is the defined basement. This annotation represents economic basement as it is the top of metasediments comprising the Proterozoic Uinta Supergroup as determined by well penetrations. The bright reflector below this is interpreted to represent granitic basement. The thick Uinta package evident on the hanging wall of the lateral ramp appears to be almost completely missing on the footwall, suggesting that, from an erosional standpoint, the relative motion of the lateral ramp must have been reversed in the past. This suggests that, in some locales, Laramide compression reactivated ancient extensional faulting and effectively inverted pre-existing structure.

Post-OVT PSTM azimuthal velocity analysis

With the relative traveltime effects of geologic dip, layer anisotropy, and isotropic velocity effectively removed from the prestack gathers via OVT PSTM, remaining traveltime distortions may be ascribed to azimuthal velocity anisotropy (up to an offset-to-depth ratio of one). This is, of course, only true if one can rule out the existence of significant rapid lateral velocity variations that would require depth imaging (Jenner, 2009).

Azimuthal velocity anisotropy manifests itself as an elliptical variation of NMO velocity with azimuth. A robust and elegant approach to azimuthal velocity analysis is by surface fitting (Jenner et al., 2001). An azimuthal NMO ellipse can be fit to the measured traveltimes via least squares fitting as the azimuthal NMO equation is linear in time^2—offset^2 space. The measured anisotropic NMO velocities can also be converted to anisotropic interval velocities using a generalized form of the Dix equation. The azimuthal traveltime differences caused by the presence of significant anisotropy can degrade the image quality of wide-azimuth surveys when ignored. If the anisotropy is measured and properly corrected, the result may not only improve the image, but also provide valuable azimuthal velocity information that can be related to local fracturing and/or stress regimes.

The migrated gathers produced by OVT prestack time migration are quite different from conventional offset gathers. Offsets are not linearly sampled and often duplicated so the gathers cannot be processed or analyzed with tools that assume constant-offset spacing. A valuable property of the surface-fitting approach to velocity analysis is that it does not require the data to have a regularized distribution as long as offsets and azimuths are sufficiently sampled to constrain an azimuthal (or isotropic) signature.

Comparison of OVT and offset PSTM imaging

Before addressing the effect that OVT PSTM has on the measured azimuthal velocity field, a comparison of the imaging results between common-offset PSTM and OVT PSTM should be made. In Figure 6, a common-offset PSTM image is presented next to an OVT PSTM image of the same line. Both images have incorporated layer anisotropy (η = 0.1) in the migration, but the common-offset PSTM has azimuthal

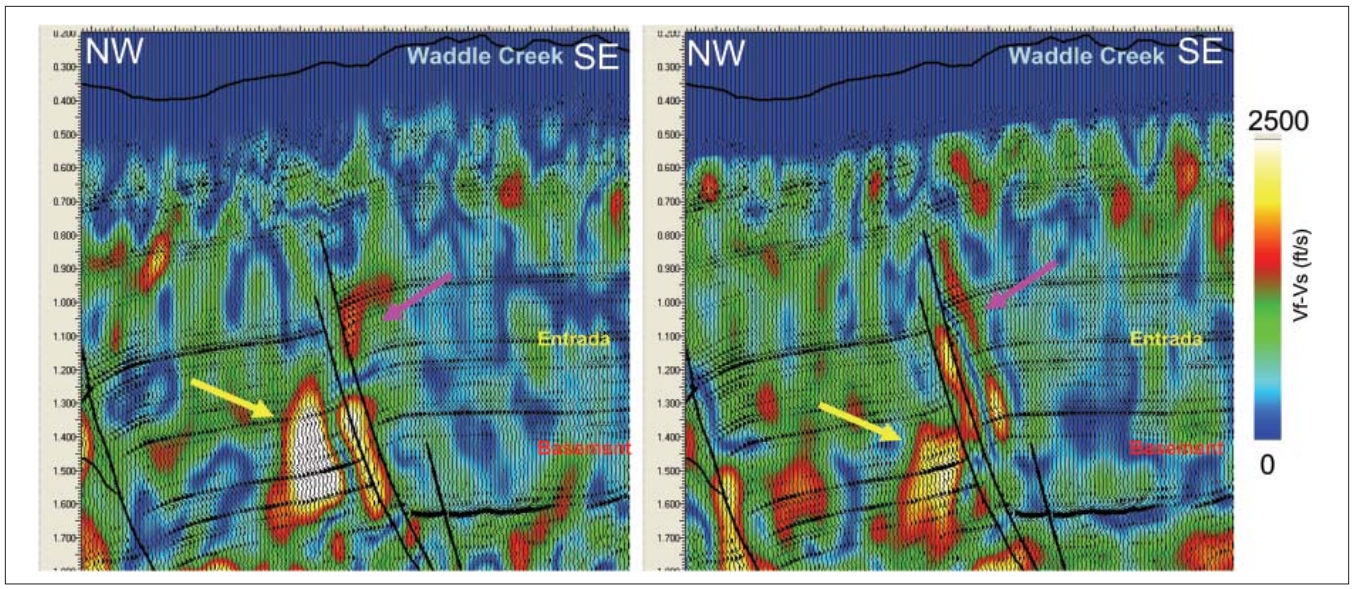

Figure 7. *Comparison of azimuthal anisotropy measured as V_{fast}-V_{slow} ft/s for unmigrated data (left) and OVT prestack time-migration data (right) on line 150. The OVT-migrated attribute appears to be better positioned relative to interpreted faulting (magenta arrow), and fault influence on this attribute is also more apparent. The deeper high V_{fast}-V_{slow} anomaly (yellow arrow) has decreased in magnitude and moved closer to the lateral ramp deformation zone, suggesting that the dip effect has been removed, but the possible influence of lateral velocity variation may remain.*

velocity analysis and correction before migration while the OVT PSTM has azimuthal velocity analysis and correction after migration. In general, the stacked images are quite comparable and differ only in slight details with no clear winner. The exception to this observation is that the OVT PSTM does not appear as coherent in the shallow section, perhaps as a result of increased sensitivity to the shallow sampling deficiencies that plague most land surveys. Further investigation into this effect is warranted.

As the migrations themselves are essentially identical except for the offset binning differences described above, it should be expected that any stack image differences would be due to whether the azimuthal corrections were measured and applied before or after the migration. Apparently the stack response is relatively insensitive to this difference; however, a detailed interpretation effort may bring to light some noteworthy attribute differences.

Azimuthal velocity attributes

An elliptical velocity field can also be thought of as a vector velocity field where the length of the long axis of the ellipse represents the magnitude of the fast velocity and the direction of the long axis represents the direction of the fast velocity, while orthogonal to that, the length of the short axis represents the magnitude of the slow velocity. As most current interpretation environments cannot readily render vector quantities, a vector velocity field is generated as separate scalar components of the vector. Volumes representing the magnitude of V_{fast}, the azimuth of V_{fast}, and the magnitude of V_{fast}-V_{slow} (the latter choice being one of convenience as V_{fast}-V_{slow} represents anisotropy magnitude) are typically output for interpretation. The interval versions of these velocity volumes are usually of the most aid to interpretation, but the rms versions have interpretive value as well.

Figure 7 shows a comparison of the interval V_{fast}-V_{slow} attribute computed before and after PSTM. Two significant differences can be seen in the vicinity of the fault deformation:

- The yellow arrow denotes a high V_{fast}-V_{slow} anomaly in the deeper portion of the footwall. This anomaly is significantly reduced in magnitude and positioned closer to the fault deformation when azimuthal velocities are computed after migration. If the long axis of the velocity ellipse and local NW-SE geologic dip are oriented in the same direction, thus reinforcing the azimuthal signature, one would expect the removal of the dip component via migration to lessen the magnitude of the azimuthal anisotropy. In addition, the migration should move it in the updip NW-SE direction (i.e., closer to the deformation zone). An examination of the V_{fast} azimuth attribute at this location indeed revealed that the V_{fast} orientation remains NW-SE after migration, suggesting that the dip effect has at least been attenuated if not removed. It should be noted that the V_{fast}-V_{slow} signature remaining after PSTM in the footwall may represent the effect of unaccounted for lateral velocity variation as raypaths imaging this location certainly spent significant time traversing the hanging wall.
- The magenta arrow denotes a significant change in the V_{fast}-V_{slow} signature within the fault deformation zone after PSTM. High V_{fast}-V_{slow} anomalies better conform to the deformation zone and support the idea that the deformation zone is characterized by en echelon faulting, as opposed to a single fault. The emergence of post-PSTM V_{fast}-V_{slow} anomalies where there were none prior to migration can be explained by dip and azimuthal anisotropy effects destructively interfering prior to migration. The V_{fast} azimuth within the deformation zone is highly variable,

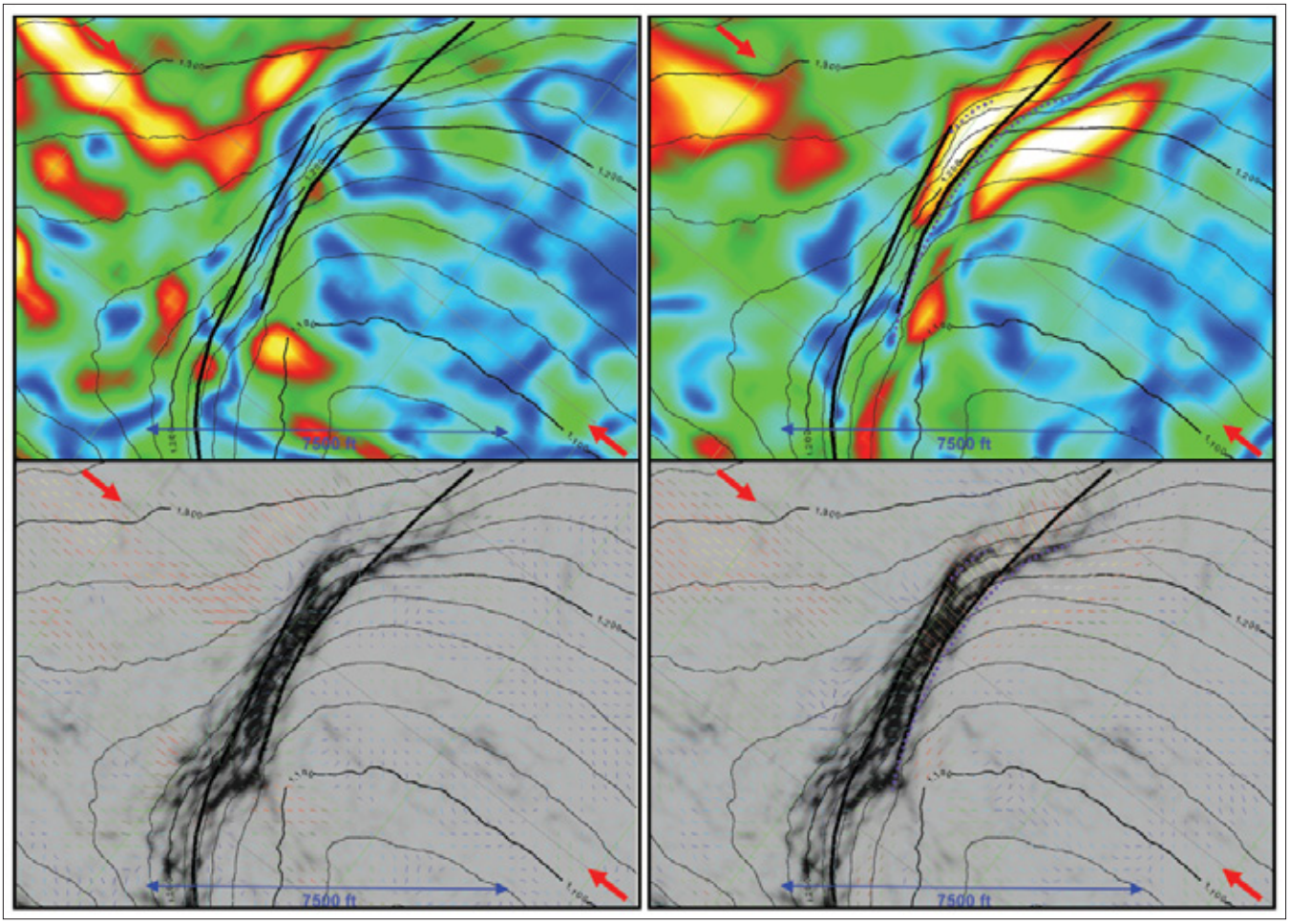

Figure 8. *Azimuthal anisotropy attributes extracted on a horizon picked at the Entrada level with stuctural overlays for reference. Top images are interval V_{fast}-V_{slow} for unmigrated (left) and OVT prestack time migration (right). Lower images are full vector representations of azimuthal anisotropy with the addition of coherency in the background. Fault interpretation adjustments suggested by OVT attributes are dashed, and red arrows denote location of line 150. Color scale is the same as in Figure 7.*

so it appears that removal of the NW-SE dip effect has effectively revealed the underlying azimuthal anisotropy associated with faulting or local flexure.

The fault interpretation appearing in Figure 7 was created solely with the image volumes available at various stages in the processing. The en echelon nature of the fault zone was recognized as imaging progressed, but proved difficult to interpret accurately in detail. Figure 8 represents a comparison of azimuthal attributes extracted at the top of the Jurassic Entrada Formation, which is situated roughly in the middle of the stratigraphic section at Waddle Creek. The top two figures show the V_{fast}-V_{slow} attribute computed before and after PSTM with structural overlays for reference. The en echelon fault interpretation of the lateral ramp deformation zone can clearly be refined (dashed faulting in Figure 8) by following trends observed in the attribute extraction. In particular, the easternmost fault should be moved slightly east and curve more dramatically in that direction, allowing the V_{fast}-V_{slow} anomalies to be more clearly identified with fault-related flexure between faults, which may indicate enhanced fracturing.

The bottom two figures show the full vector representation of the extracted interval azimuthal velocity field before and after PSTM as icons overlain on structure and coherency extraction. The coherency clearly supports an adjustment of the fault geometries consistent with the trends seen in V_{fast}-V_{slow}. The full vector representation is presented here as icon length equaling the magnitude of V_{fast}, icon color as the magnitude of V_{fast}-V_{slow}, and icon orientation of V_{fast} azimuth. The various (relative) combinations of these components summarized in the icons may give the interpreter clues to the interplay of local structure, fracturing, and stresses that can contribute to enhancing production in a target reservoir (Simon, 2005).

Conclusions

The Durham Ranch 3D survey acquired spatially dense, high-quality P-wave data in a very challenging surface environment. Traditional isotropic processing of these data does not properly image the details of the Waddle Creek structure that are important to prospecting for unconventional reservoirs. Incorporation of layer anisotropy in prestack time migration considerably improved the imaging of the lateral

ramp deformation zone bounding the field on the northwest; performing the prestack time migration in the offset vector domain (OVT) allowed more accurate azimuthal velocity analysis in the presence of structure. The resulting azimuthal attributes can better help the interpreter identify areas of enhanced natural fracturing and design more favorable fracture stimulation strategies as they are now more in agreement with the structural framework.

The improved azimuthal velocity field can also be incorporated into the prestack time migration in the attempt to achieve further imaging improvement, but this has yet to be performed on Durham Ranch. Additional investigation of these data will hopefully reveal methods to improve the shallow response of OVT prestack time migration and eventually lead to resolution of any remaining inaccuracies due to rapid lateral velocity change that can only be accomplished with prestack depth migration.

The converted-wave data that were acquired during the Durham Ranch 3D shoot are currently being evaluated. The images and attributes provided by these data may provide further insight into the anisotropy/fracture story.

Suggested reading. "Preserving azimuthal velocity information: Experiences with cross-spread noise attenuation and offset vector tile preSTM" by Calvert et al. (SEG 2008 *Expanded Abstracts* and online tutorial at *http://pd.global.playstream.com/i-o/progressive/Offset_Vector_Tiling/OVT_Calvert_31009.wmv*). "Cableless system meets challenge of acquiring seismic to define subtle fractures in complex shale" by Chitwood et al. (*First Break*, 2009). "Data example and modeling study of P-wave azimuthal anisotropy potentially caused by isotropic velocity heterogeneity" by Jenner (*First Break*, 2009). "A new method for azimuthal velocity analysis and application to a 3D survey, Weyburn Field, Saskatchewan, Canada" by Jenner et al. (SEG 2001 *Expanded Abstracts*). "Uncertainty implications in azimuthal velocity analysis" by Lynn (SEG 2007 *Expanded Abstracts*). Stress and Fracture Characterization in a Shale Reservoir, North Texas, Using Correlation Between New Seismic Attributes and Well Data by Simon (Master's thesis, University of Houston, 2005). "Interpreting seismic data in the presence of azimuthal anisotropy; or azimuthal anisotropy in the presence of seismic interpretation" by Williams and Jenner (*TLE*, 2002). Contact the author for an expanded list of relevant articles. TLE

Acknowledgments: The authors thank East Resources for their participation and support of this work. In addition, we thank the many people at GX Technology and ION that helped with this project.

Corresponding author: scott.schapper@iongeo.com